

Microstructural Evolution and Magnetic Properties of Aged CoNiGaAl Shape Memory Alloy

N. EL-BAGOURY^{1,2,4} and M.M. RASHAD³

1.—Chemistry Department, Faculty of Science, TAIIF University, El-Haweyah, El-Taif, Saudi Arabia. 2.—Casting Technology Lab, Manufacturing Technology Department, CMRDI, Central Metallurgical Research and Development Institute, Helwan, Cairo, Egypt. 3.—Head of Electronic Materials Lab, Advanced Materials Department, CMRDI, Central Metallurgical Research and Development Institute, Helwan, Cairo, Egypt. 4.—e-mail: nader_elbagoury@yahoo.com

A study on the influence of aging heat treatment conditions at 823 K for 3 h, 24 h, and 120 h, on microstructure, martensitic transformation, and magnetic and mechanical properties of $\text{Co}_{50}\text{Ni}_{23}\text{Ga}_{27-X}\text{Al}_X$ alloys ($X = 0$ and 1 at.%) was performed by using x-ray diffraction (XRD) analysis, optical microscopy (OM), energy-dispersive spectrometer (EDS), differential scanning calorimeter (DSC), and vibrating sample magnetometer (VSM). The results show that the microstructure of both aged alloys consists of martensite and fcc second γ phase in addition to ordered cubic gamma prime (γ') phase precipitates in martensite. The martensitic transformation temperature peak (M_p) elevates with prolonging aging time and decreasing valence electron concentration (e_v/a). Saturation magnetization (M_s) decreases, whereas both remanence magnetization (M_r) and coercivity (H_c) increase with aging time. Meanwhile, the aging time enhances the hardness property (H_v) of the investigated alloys.

INTRODUCTION

Recently, more interest has been generated in the ferromagnetic shape memory alloys (FMSMAs) because of their various applications such as sensors and actuators materials.¹ A lot of FMSMAs like NiMnGa^{2–5} exhibit a magnetically induced shape memory effect and excellent thermal stability.⁶ However, this system of alloys has some drawbacks, mainly originating from the loss of Mn. It causes severe brittleness in polycrystalline alloys in addition to high segregation in single crystal alloys that limits its applications.^{7,8} Therefore, several trials have been made to develop new systems such as NiFeGa, CoNiAl, and CoNiGa to avoid the demerits of NiMnGa alloys. Accordingly, in comparison with NiMnGa alloys, the new developed group of the FMSMAs in the Co-Ni-Ga alloy system located in the two-phase B2 + γ (martensite + γ) region is characterized by good ductility due to the γ phase in its microstructure.^{9–12} The microstructure with a higher volume fraction of γ phase, soft phase, at the expense of martensite, hard phase, has higher ductility.

A lot of studies have reported that heat treatment conditions seriously influence the microstructure, martensitic transformation, and magnetic and mechanical properties of various FMSMAs.^{13–15} In addition to heat treatment influence, Al addition to the CoNiGa system can alter its volume fraction of martensite and γ phase, martensitic transformation temperature peak (M_p), and saturation magnetization (M_s).

Additionally, it is worth mentioning in this context that valence electron concentration (e_v/a) is the most important factor influencing structure, as well as M_p , mechanical and magnetic properties such as M_s , remanence magnetization (M_r), and coercivity (H_c).^{16,17} Furthermore, (e_v/a) indicates the number of all electrons in the alloys per number of atoms. Consequently, the following equation is used to calculate this ratio, e_v/a , based on the atomic fractions of the alloying elements in the alloy:¹⁶

$$e_v/a = f_1e_v^1 + f_2e_v^2 + f_3e_v^3 \quad (1)$$

where f is the atomic fraction and e_v is the number of valence electrons of the elements in the alloy.^{18–20} There are two opposite opinions that

control the relationship between M_p and e_v/a . For instance, many researchers have reported that the M_p is in direct relation with e_v/a .^{16,21–23} Otherwise, others have indicated that it is an inverse relationship between M_p and e_v/a .^{24–26} Moreover, it is found that the magnetic saturation measurements are affected by the e_v/a . Indeed, the increase in e_v/a causes a decrease in M_s .¹⁷

Herein, in the present study, the influence of aging conditions and Al doping on the microstructure evolution, martensitic transformation, and mechanical and magnetic properties of $\text{Co}_{50}\text{Ni}_{23}\text{Ga}_{27-X}\text{Al}_X$ alloys is investigated.

EXPERIMENTAL PROCEDURES

The dual phase of ($\beta + \gamma$) $\text{Co}_{50}\text{Ni}_{23}\text{Ga}_{27-X}\text{Al}_X$ alloys ($X = 0$ and 1 at.%) was prepared from the starting materials of 99.99 wt.% Co, 99.99 wt.% Ni, and 99.99 wt.% Ga by arc-melting pure elements under an argon atmosphere in a water-cooled copper crucible. To lower segregation and ensure homogenization as much as possible, the cast alloys used in this investigation were melted four times. After being solutionized at 1273 K for 24 h for both alloys, under a controlled atmosphere of He, these two specimens were sliced into small-sized parts, which were then aged at 823 K for various periods 3 h, 24 h, and 120 h followed by iced water quenching (WQ). The microstructure was evaluated by an optical microscope (OM) (MEIJI TECHNO) fitted with a digital camera and a scanning electron microscope (SEM—JEOL JSM5410). The equilibrium phase composition was detected by an energy x-ray dispersive spectroscopy (EDS) attached to SEM. The crystalline phases in the different samples were distinguished by using x-ray diffraction (XRD) on the Bruker axis D8 diffractometer using Cu K α ($\lambda = 1.5406$) radiation with a step scanning in the 2θ range of 30° to 100° . The peak of martensitic transformation temperatures (M_p) was determined by differential scanning calorimetry (Netzsch Leading Thermal Analysis DSC 204 F1) at heating and cooling rates of 10 K/min. Magnetic properties were measured as well by using a vibrating sample magnetometer (VSM; lakeshore 7400; USA). Hardness values were determined by using a Leco Vickers Hardness Tester LV800AT with 31.25 Kg_f.

RESULTS AND DISCUSSION

Crystal Structure

To investigate the influence of aging heat treatment conditions on the structure and to identify the different phases found in $\text{Co}_{50}\text{Ni}_{23}\text{Ga}_{27}$ and $\text{Co}_{50}\text{Ni}_{23}\text{Ga}_{26}\text{Al}_1$ alloys, x-ray diffraction measurements were performed at room temperature. There are six XRD patterns, as shown in Fig. 1; each alloy was represented by three XRD patterns according to aging at 823 K for various aging times: 3 h, 24 h, and 120 h. The XRD results reveal the crystal

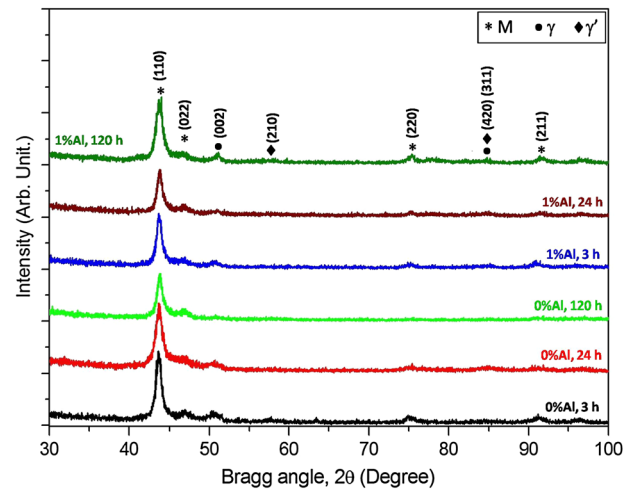


Fig. 1. XRD patterns of the aged $\text{Co}_{50}\text{Ni}_{23}\text{Ga}_{27}\text{Al}_0$ and $\text{Co}_{50}\text{Ni}_{23}\text{Ga}_{26}\text{Al}_1$ alloys.

structures of the present phases. These phases were determined to be $L1_0$ for martensite phase, $A1$ for γ phase (disordered fcc), and $L1_2$ for γ' phase (ordered cubic). The main reflection (110) was indexed with the tetragonal structure for the parent phase: martensite.²⁵ Moreover, there are some other peaks such as (022), (220), and (211) that indicate the presence of martensite phase as well. Furthermore, γ phase is represented in Fig. 1 by diffraction planes (002) and (420); however, (210) and (311) planes belong to the γ' phase.

Microstructure Evolution

Figure 2 depicts the microstructures, observed by optical microscope, of both $\text{Co}_{50}\text{Ni}_{23}\text{Ga}_{27}$ and $\text{Co}_{50}\text{Ni}_{23}\text{Ga}_{26}\text{Al}_1$ alloys where (a), (b), and (c) represent the microstructures of $\text{Co}_{50}\text{Ni}_{23}\text{Ga}_{27}$ alloys that aged at 823 K for 3 h, 24 h, and 120 h, respectively, and (d), (e), and (f) illustrate the counterpart microstructures of $\text{Co}_{50}\text{Ni}_{23}\text{Ga}_{26}\text{Al}_1$ alloy. The microstructures of both investigated alloys aged with different heat treatment conditions are composed of martensite, γ phase in addition to particles of γ' phase that precipitated in martensite phase, as evinced in Fig. 3. The γ phase and its volume fraction (V_f) in the microstructures of $\text{Co}_{50}\text{Ni}_{23}\text{Ga}_{27}$ alloy, (a), (b), and (c), are coarser and higher than that in the counterpart microstructures of $\text{Co}_{50}\text{Ni}_{23}\text{Ga}_{26}\text{Al}_1$ alloy, (d), (e), and (f). Meanwhile, the V_f of the γ phase in both $\text{Co}_{50}\text{Ni}_{23}\text{Ga}_{27}$ and $\text{Co}_{50}\text{Ni}_{23}\text{Ga}_{26}\text{Al}_1$ alloys decreases with prolonging the aging time. Obviously, the V_f of the γ phase diminishes in both alloys with increasing the aging time from 3 h and 24 to 120 h. In addition, γ' phase is precipitated in the martensite phase in all microstructures of the aged specimens. These particles of γ' phase got coarser as the aging time increased, as described in Fig. 3.

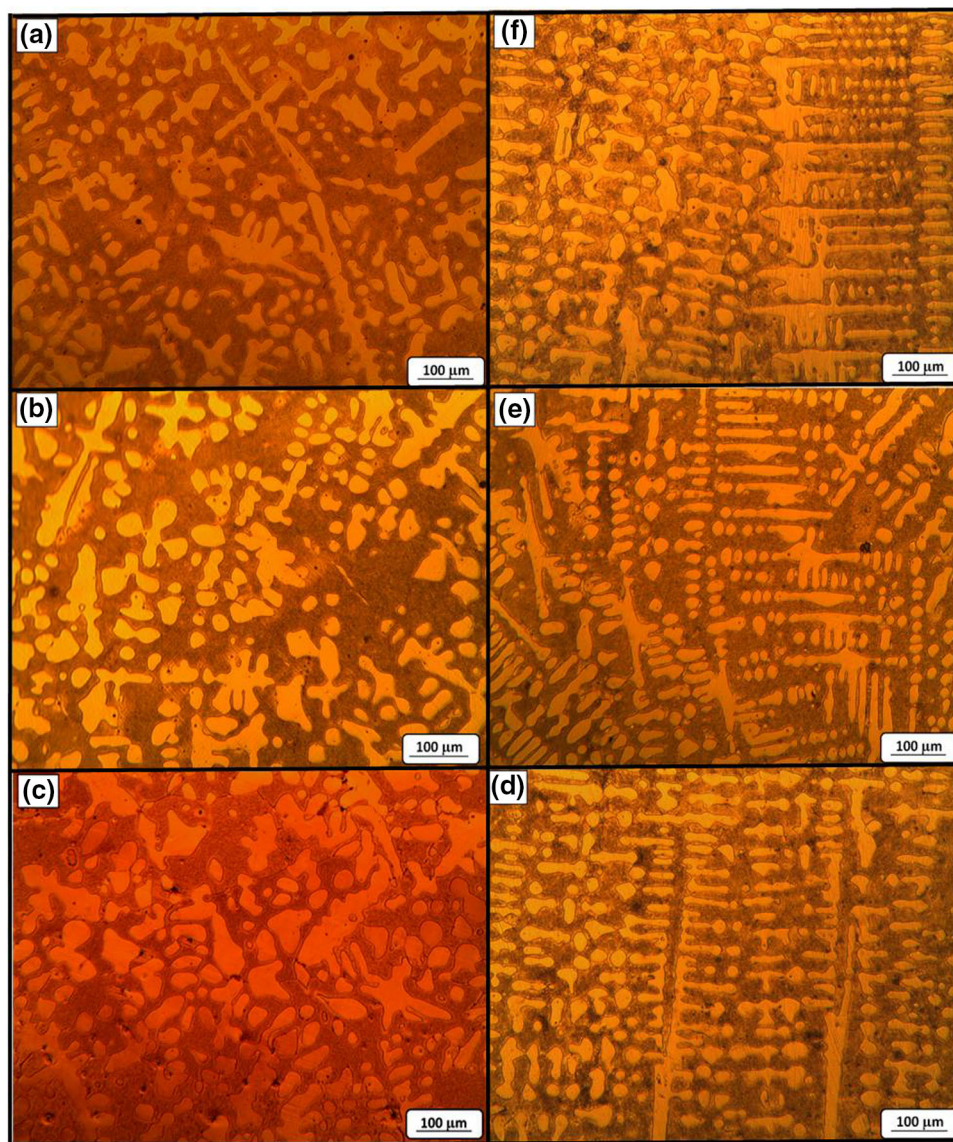


Fig. 2. Microstructure of $\text{Co}_{50}\text{Ni}_{23}\text{Ga}_{27}$ alloys aged at 550°C for (a) 3 h, (b) 24 h, and (c) 120 h and $\text{Co}_{50}\text{Ni}_{23}\text{Ga}_{26}\text{Al}_1$ alloys aged at 823 K for (d) 3 h, (e) 24 h, and (f) 120 h.

The distribution of the alloying elements, Co, Ni, and Ga, in the martensite and γ phases found in the microstructure of $\text{Co}_{50}\text{Ni}_{23}\text{Ga}_{27}$ alloy aged at 823 K for 120 h is shown in Fig. 4. Chemical distribution provides a clear image about the heat treatment influence on segregation of alloying elements, which in turn affect the presence and the volume fraction of different phases, such as gamma (γ), gamma prime (γ'), and martensite, found in the investigated microstructures. Moreover, chemical distribution explains the anisotropy of the physical and mechanical properties. The martensite phase has higher content of both Ga and Ni elements; however, the γ phase is rich in Co element. Moreover, the microchemical analysis of martensite and γ phases is recorded in Table I, whereas Table II demonstrates the microchemical analysis of γ' phase. It is

noticeable that (γ') phase is Co based with higher Al content, as presented in Table II. Additionally, this table contains the percentage of error for the measurements of microchemical analyses of alloying elements: Co, Ni, Ga, and Al.

In addition, the influence of aging treatment conditions on the martensite transformation temperatures (T_m) is investigated. As the aging time increases, the T_m for both $\text{Co}_{50}\text{Ni}_{23}\text{Ga}_{27}$ and $\text{Co}_{50}\text{Ni}_{23}\text{Ga}_{26}\text{Al}_1$ alloys increase as deduced in Table I. Meanwhile, the T_m for $\text{Co}_{50}\text{Ni}_{23}\text{Ga}_{27}$ alloys is lower than that of $\text{Co}_{50}\text{Ni}_{23}\text{Ga}_{26}\text{Al}_1$ alloys. Thus, Al is increasing the martensitic transformation temperature when it is added on account of Ga.²⁶ Moreover, one can note that T_m is very sensitive to the chemical composition of the matrix phase, which is martensite; however, there is a percentage of error

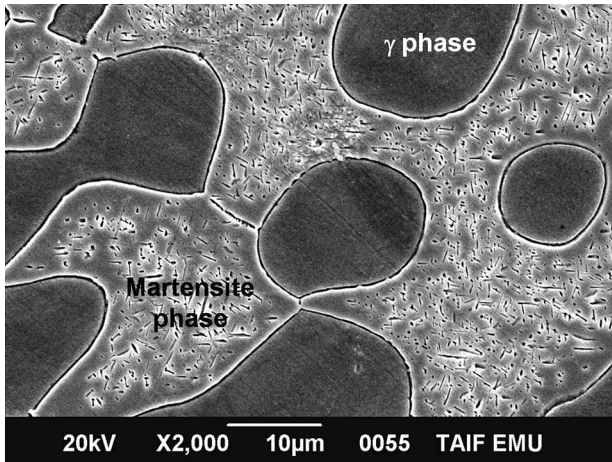


Fig. 3. Parent: martensite phase and γ phase and precipitation of γ phase in martensite in the microstructure of $\text{Co}_{50}\text{Ni}_{23}\text{Ga}_{27}\text{Al}_1$ alloy aged for 120 h.

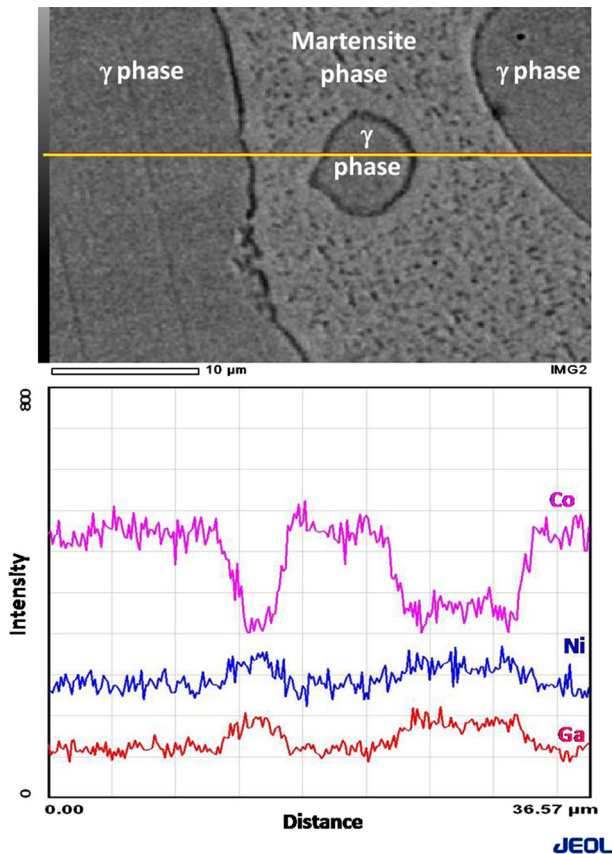


Fig. 4. Line analysis through γ and martensite phases in $\text{Co}_{50}\text{Ni}_{23}\text{Ga}_{27}\text{Al}_1$ alloy aged for 120 h.

in any experimental measurements that should be taken into account; for example, see Table II. Accordingly, the Al percentage increases, while the Co content decreases in the matrix, martensite,

with aging time. Al and Ga preferably segregate to martensite, while Co selectively separates into the γ phase.⁶

It is obvious that T_m increases with the increase of Ga at.%,¹ however, it is decreased by increasing the Co content⁶ in the matrix of $\text{Co}_{50}\text{Ni}_{23}\text{Ga}_{27}$ alloy, as shown in Table I. In addition to the effect of Ga and Co, the increase of Al (at.%) elevates the T_m of the $\text{Co}_{50}\text{Ni}_{23}\text{Ga}_{26}\text{Al}_1$.²⁵

The chemical composition of the matrix affect on the T_m is represented by the valence electron concentration (e_v/a). A lot of researchers investigated the relationship between T_m and (e_v/a). This relationship is a controversial issue, where some researchers have indicated that it is a direct relationship.^{1,16,21,22} However, others have confirmed that it is an inverse relationship.^{6,23,24} The obtained results in the present study support the latter point of view.

Mehrdad and Yong²⁷ studied this relation in detail. They categorized alloys into low ($e_v/a < 5$), medium ($5 \leq e_v/a \leq 7.50$), and high ($e_v/a > 7.50$) valence electron groups. As shown in Table I, the values of (e_v/a) in this study belong to the medium category. In this category, according to Mehrdad and Young, the relationship between T_m and (e_v/a) is an inverse relation that coincides with the results of this study.

Magnetic Properties

The effect of aging time on the magnetic properties of the CoNiGaAl alloys was performed at room temperature under an applied field of 15 kOe using a vibrating sample magnetometer (VSM). These measurements were carried out at room temperature under an applied field of 15 kOe. Plots of magnetization (M) as a function of applied field (H) for the $\text{Co}_{50}\text{Ni}_{23}\text{Ga}_{27}$ and $\text{Co}_{50}\text{Ni}_{23}\text{Ga}_{26}\text{Al}_1$ alloys aged at 823 K for 3 h, 24 h, and 120 h are shown in Fig. 5.

The change on saturation magnetization (M_s), remanence magnetization (M_r), and coercivity (H_c) for $\text{Co}_{50}\text{Ni}_{23}\text{Ga}_{27}\text{Al}_0$ and $\text{Co}_{50}\text{Ni}_{23}\text{Ga}_{26}\text{Al}_1$ alloys obtained at room temperature are shown in Fig. 6. It is noticeable that M_s for both $\text{Co}_{50}\text{Ni}_{23}\text{Ga}_{27}\text{Al}_0$ and $\text{Co}_{50}\text{Ni}_{23}\text{Ga}_{26}\text{Al}_1$ alloys aged at 823 K for 3 h is found to be 124.15 emu/g and 58.36 emu/g, respectively. By prolonging the aging time to 24 h and further to 120 h, the M_s for both aged alloys is found to minify into 65.52 emu/g and 50.61 emu/g and then to 53.07 emu/g and 46.16 emu/g, respectively.

All the measured magnetic properties for aged $\text{Co}_{50}\text{Ni}_{23}\text{Ga}_{27}\text{Al}_0$ alloys are higher than in $\text{Co}_{50}\text{Ni}_{23}\text{Ga}_{26}\text{Al}_1$ alloys, as shown in Fig. 6. Additionally, the M_s decreased for both aged $\text{Co}_{50}\text{Ni}_{23}\text{Ga}_{27}\text{Al}_0$ and $\text{Co}_{50}\text{Ni}_{23}\text{Ga}_{26}\text{Al}_1$ alloys with aging time; however, both M_r and H_c are increased for aged $\text{Co}_{50}\text{Ni}_{23}\text{Ga}_{27}\text{Al}_0$ and $\text{Co}_{50}\text{Ni}_{23}\text{Ga}_{26}\text{Al}_1$ alloys as the aging time increases.

Table I. Microchemical analyses of martensite phase, electron concentration in matrix (e_v/a), and martensite transformation temperature (T_m) of the investigated alloys

Alloy	Composition of martensite (at.%)				(e_v/a)	T_m (°C)
	Co	Ni	Ga	Al		
Al ₁ , 3 h	42.24	27.33	29.16	1.28	7.4478	89
Al ₁ , 24 h	41.93	27.36	29.34	1.37	7.4310	94
Al ₁ , 120 h	40.32	28.20	29.99	1.49	7.3932	112
Al ₀ , 3 h	41.52	26.69	31.79	0.00	7.3595	78
Al ₀ , 24 h	41.34	26.81	31.85	0.00	7.3568	86
Al ₀ , 120 h	41.09	26.95	31.95	0.00	7.3516	97

Table II. Microchemical Analyses of γ' Phase

Alloy	Composition of γ' phase (at.%)			
	Co	Ni	Ga	Al
1% Al, 120 h	58.62	22.52	17.45	1.41
% Error	0.26	0.32	0.69	0.46

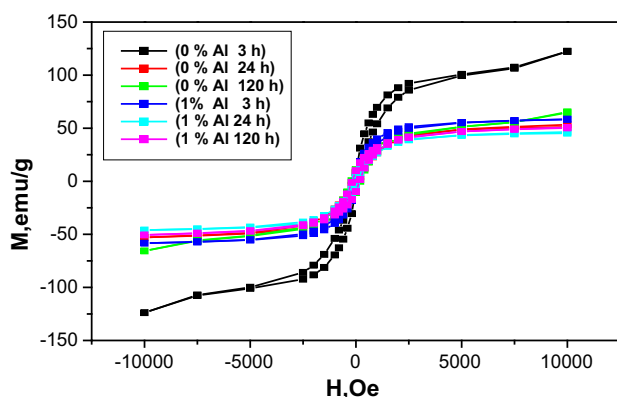


Fig. 5. Effect of aging time on the M-H hysteresis loop of CoNiGaAl alloys.

The main two phases in the microstructures of the investigated alloys are the martensite and the γ phase. These two phases have different magnetic properties, where the γ phase, a Co-rich phase, has larger magnetization compared to martensite phase.²⁸ Moreover, the Co additions increase the V_f of the γ phase and make it more stable as well as increase its saturation magnetization that was confirmed by Liu et al.⁶ However, Al segregates preferably to the martensite phase and increases its V_f and lowering of the M_s of aged alloys.

The M_s values of aged Co₅₀Ni₂₃Ga₂₆Al₁ alloys are lower than that of Co₅₀Ni₂₃Ga₂₇Al₀ alloys according to the diminishing in the V_f of the γ phase in the

microstructure of Co₅₀Ni₂₃Ga₂₇Al₀ alloys than of Co₅₀Ni₂₃Ga₂₆Al₁ alloys due to the increase in the Al (at.%).²⁵ Furthermore, the decrease in the saturation magnetization for both aged Co₅₀Ni₂₃Ga₂₇Al₀ and Co₅₀Ni₂₃Ga₂₆Al₁ alloys with aging time originated from the decrease in the V_f of the γ phase due to the decrease in the Co (at.%).⁶

Mechanical Properties

The influence of the prolonging time of the aging process on the hardness of the investigated alloys is elucidated in Fig. 7. The hardness values for the specimens aged at 823 K for 3 h, 24 h, and 120 h of Co₅₀Ni₂₃Ga₂₆Al₁ alloy, 270, 307, and 353 HV₃₀, are higher than the corresponding specimens for Co₅₀Ni₂₃Ga₂₇Al₀ alloys, 262, 277, and 341 HV₃₀, respectively. Hardness measurements for the both investigated alloys are in a direct relationship with aging time, whereas as the aging time increases, the hardness values increase.

The increase in the hardness measurement for both Co₅₀Ni₂₃Ga₂₇Al₀ and Co₅₀Ni₂₃Ga₂₆Al₁ alloys with aging time could be due to the increase of the V_f of martensite at the expense of V_f of the γ phase. In the same direction, hardness measurements are enhanced with aging time as the result of the precipitation of the γ' phase in both aged alloys.

In comparison with the counterpart specimens of Co₅₀Ni₂₃Ga₂₇ alloys, Co₅₀Ni₂₃Ga₂₆Al₁ alloys have higher hardness values because of the higher V_f of the martensite phase and a finer structure than in Co₅₀Ni₂₃Ga₂₇ alloys.

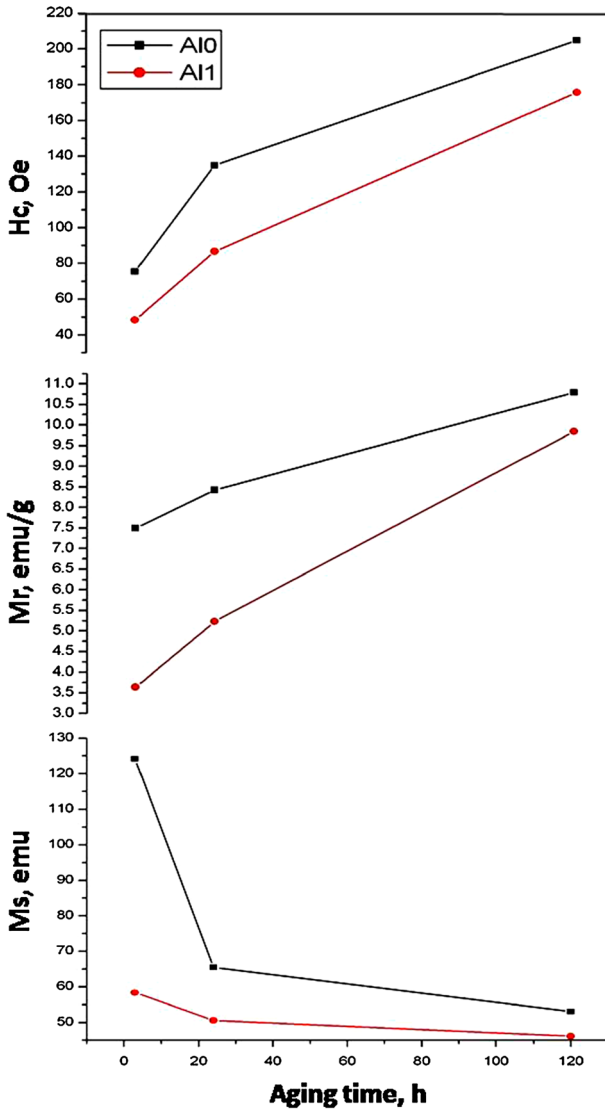


Fig. 6. Influence of aging time on the saturation magnetization (M_s), remanence magnetization (M_r), and coercivity (H_c) of CoNiGaAl alloys.

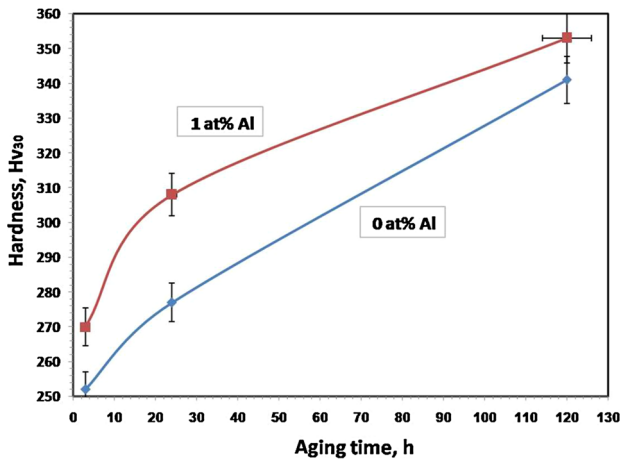


Fig. 7. Hardness measurements versus aging time.

CONCLUSION

The microstructure, martensitic transformation, and magnetic and mechanical properties of $\text{Co}_{50}\text{Ni}_{23}\text{Ga}_{27-x}\text{Al}_x$ alloys that aged at 823 K with various aging times of 3 h, 24 h, and 120 h were investigated. The obtained results are as follows:

1. The microstructure is composed of Ga-rich martensite, as a parent phase, Co-rich γ phase, as well as precipitation of γ' phase particles for both $\text{Co}_{50}\text{Ni}_{23}\text{Ga}_{27}\text{Al}_0$ and $\text{Co}_{50}\text{Ni}_{23}\text{Ga}_{26}\text{Al}_1$ alloys.
2. V_f of the γ phase in the $\text{Co}_{50}\text{Ni}_{23}\text{Ga}_{27}\text{Al}_0$ alloy is higher than that in the $\text{Co}_{50}\text{Ni}_{23}\text{Ga}_{26}\text{Al}_1$ alloy. Moreover, the V_f value of the γ phase is decreased by prolonging the aging time for both alloys.
3. The martensitic transformation temperature T_m is elevated as the aging time increases; however, it decreases as the electron concentration (e_v/a) increases.
4. The magnetic parameters M_s , M_r , and H_c for the $\text{Co}_{50}\text{Ni}_{23}\text{Ga}_{27}\text{Al}_0$ alloy are higher than those for the $\text{Co}_{50}\text{Ni}_{23}\text{Ga}_{26}\text{Al}_1$ alloy in all aging conditions. Saturation magnetization (M_s) values decrease, whereas remanence magnetization (M_r) and coercivity (H_c) values increase as the aging time increases.
5. Hardness measurements for both alloys are increased with aging time. In comparison with the $\text{Co}_{50}\text{Ni}_{23}\text{Ga}_{26}\text{Al}_1$ alloy, the $\text{Co}_{50}\text{Ni}_{23}\text{Ga}_{27}$ alloy has lower hardness values.

REFERENCES

1. E. Dogan, I. Karaman, Y.I. Chumlyakov, and Z.P. Luo, *Acta Mater.* 59, 1168 (2011).
2. K. Ulakko, J.K. Huang, C. Kantner, R.C.O. Handly, and V.V. Kokorin, *Appl. Phys. Lett.* 69, 1966 (1996).
3. R.C.O. Handly, *J. Appl. Phys.* 83, 3263 (1998).
4. V.A. Chernenko, *Scripta Mater.* 40, 523 (1999).
5. S.J. Murray, M. Marioni, S.M. Allen, R.C.O. Handly, and T.A. Lograsso, *Appl. Phys. Lett.* 77, 886 (2000).
6. J. Liu, H.X. Zheng, M.X. Xia, Y.L. Huang, and J.G. Li, *Scripta Mater.* 52, 935 (2005).
7. Y. Li, Y. Xin, C.B. Jiang, and H.B. Xu, *Scripta Mater.* 51, 849 (2004).
8. D.L. Schlagel, Y.L. Wu, W. Zhang, and T.A. Lograsso, *J. Alloy. Compd.* 312, 77 (2000).
9. K. Oikawa, L. Wulff, T. Lijima, F. Gejima, T. Ohmori, A. Fujiata, K. Fukamichi, R. Kainuma, and K. Ishida, *Appl. Phys. Lett.* 79, 3290 (2001).
10. M. Wuttig, J. Li, and C. Craciunescu, *Scripta Mater.* 44, 2393 (2001).
11. K. Oikawa, T. Ota, Y. Sutou, T. Ohmori, R. Kainuma, and K. Ishida, *Metall. Mater. Trans.* 43, 2360 (2002).
12. K. Oikawa, T. Ota, F. Gejima, T. Ohmori, R. Kainuma, and K. Ishida, *Metall. Mater. Trans.* 42, 2472 (2001).
13. D.L. Schlagel, T.A. Lograsso, and A.O. Pecharsky, *Mater. Res. Soc. Symp. Proc.* 785, 219 (2004).
14. J. Liu, L. Jian, X.X. Ming, X.Z. Hong, and G.L. Jian, *J. Alloys Compd.* 417, 96 (2006).
15. Y. Kishi, C. Craciunescu, M. Sato, T. Okazaki, Y. Furuya, and M. Wuttig, *J. Magn. Magn. Mater.* 262L, 186 (2003).
16. K. Yamaguchi, S. Ishida, and S. Asano, *Metall. Mater. Trans.* 44, 204 (2003).

17. M. Kk and Y. Aydođdu, *J. Supercond. Nov Magn.* 26, 1691 (2013).
18. M. Zarinejad and Y. Liu, *Adv. Funct. Mater.* 18, 2789 (2008).
19. T. Krenke, X. Moya, S. Aksoy, M. Acet, P. Entel, L. Manosa, A. Planes, Y. Elerman, A. Ycel, and A.E.F. Wassermann, *J. Mag. Magn. Mater.* 310, 2788 (2007).
20. S.E. Kulkavov, S.V. Ereemeev, and S.S. Kulkov, *Solid State Commun.* 130, 793 (2004).
21. J. Liu, M. Xia, Y. Huang, H.X. Zheng, and J. Li, *J. Alloy. Compd.* 417, 96 (2006).
22. X.F. Dai, H.Y. Wang, G.D. Liu, Y.G. Wang, X.F. Duan, J.L. Chen, and G.H. Wu, *J. Phys. D Appl. Phys.* 39, 2886 (2006).
23. Z.H. Liu, M. Zhang, W.Q. Wang, W.H. Wang, J.L. Chen, G.H. Wu, F.B. Meng, H.Y. Liu, B.D. Liu, J.P. Qu, and Y.X. Li, *J. Appl. Phys.* 92, 5006 (2002).
24. N. El-Bagoury, Q. Mohsen, M.A. Kaseem, and M.M. Hessian, *Metall. Mater. Int.* 19, 991 (2013).
25. N. El-Bagoury and M.A. Kaseem, *Metallogr. Microstruct. Anal.* 4, 403 (2015).
26. C. Craciunescu, Y. Kishi, T.A. Lograsso, and M. Wutting, *Scripta Mater.* 47, 285 (2002).
27. M. Zarinejad and Y. Liu, *Shape Memory Alloys: Manufacture, Properties and Applications*, ed. H.R. Chen (Nova Science Publishers, Inc., Hauppauge, 2010), pp. 339–360.
28. H. Fu, H.J. Yu, B.H. Teng, X.Y. Zhang, and X.T. Zu, *J. Alloy. Compd.* 474, 595 (2009).